

Modulation of the Lifetime of Water Bound to Lanthanide Metal Ions in Complexes with Ligands Derived from 1,4,7,10-Tetraazacyclododecane Tetraacetate (DOTA)

by Shanrong Zhang^a), Xiuyan Jiang^b), and A. Dean Sherry^{*b})^c)

^a) Department of Radiology, University of Washington Medical Center, P. O. Box 357115, 1959 N. E. Pacific Street, Seattle, WA 98195-7115, U.S.A.

^b) Department of Chemistry, University of Texas at Dallas, P. O. Box 830688, Richardson, TX 75083-0688, U.S.A.

^c) Rogers Magnetic Resonance Center, Department of Radiology, University of Texas Southwestern Medical Center, 5323 Harry Hines Blvd., Dallas, TX 75390-9085, U.S.A.

(phone: +1-972-883-2907; fax: +1-972-883-2925; e-mail: sherry@utdallas.edu)

This paper is written in celebration of the 65th birthday of Professor *André E. Merbach*

A series of di- and tetraamide derivatives of DOTA were synthesized, and their lanthanide(III) complexes were examined by multinuclear ¹H-, ¹³C-, and ¹⁷O-NMR spectroscopy, and compared with literature data of similar, known complexes (*Table*). All ligands formed structures similar to the parent [Ln^{III}(DOTA)]⁻ complexes, with four N-atoms and four O-atoms from DOTA and one O-atom from the inner-sphere water molecules. Interestingly, the lifetimes τ_M of the inner-sphere, metal-bound water molecules vary widely, ranging from nano- to milliseconds, depending on the identity of the pendent amide side chains. In general, positively charged [Ln^{III}(DOTA-tetraamide)]³⁺ complexes display the longest residence times (high τ_M values), while complexes with additional charged functional groups on the extended amides display much smaller τ_M values, even when the side groups are not directly coordinated to the central Ln³⁺ ions. The design of novel [Ln^{III}(DOTA-tetraamide)]³⁺ complexes with a wide, tunable range of τ_M values is of prime importance for the application of fast-responding, paramagnetic chemical-exchange-saturation-transfer (PARACEST) imaging agents used for the study of physiological and metabolic processes.

1. Introduction. – Magnetic-resonance imaging (MRI) has rapidly become one of the dominant imaging modalities used in clinical medicine. In addition to providing exquisite high-resolution anatomical images, MRI can also provide insights into abnormal tissue structures (MT imaging) and flow (angiography). Injection of a drug to further enhance image contrast is currently practiced in about one third of all clinical MRI studies. Low-molecular-weight gadolinium (Gd³⁺) complexes that feature a single inner-sphere-bound water molecule in rapid exchange with bulk tissue water are most commonly used as contrast agents (CA) [1]. The relaxation efficiency or relaxivity (symbolized by r_1) of typical Gd³⁺-based CA currently in use is relatively low ($r_1 \approx 4 \text{ mM}^{-1} \text{ s}^{-1}$), much lower than theoretically possible (*ca.* $120 \text{ mM}^{-1} \text{ s}^{-1}$) [2]. Such low relaxivity values do not limit the use of CA as bulk extracellular relaxation agents, but will likely become a limitation when applying MRI to molecular imaging of selected biological targets or specific cellular events [3].

During the early years of CA development, it was assumed that the rate of exchange of water molecules bound to lanthanide (Ln) ions in complexes was fast enough not to impinge upon relaxivity. However, more-recent studies, catalyzed by the pioneering

work of *Andre Merbach* and his group, have revealed that this is not, in fact, the case. For example, the water residence lifetimes (τ_M) of two common clinical agents, $[\text{Gd}^{\text{III}}(\text{DTPA})]^{2-}$ and $[\text{Gd}(\text{DOTA})]^-$, are 303 and 240 ns, respectively [4][5], some two orders of magnitude higher than that of the aqua Gd^{3+} ion [6–11]. *Merbach* and co-workers [12] also discovered that τ_M of bound water in the neutral diamide complex $[\text{Gd}^{\text{III}}(\text{DTPA})(\text{BMA})]^0$, was even higher, *ca.* 2.2 μs . It is now clear that CA that undergo such a slow water exchange become a limitation in our attempts to create high-relaxivity contrast agents. Subsequent physical studies, inspired by the work of *Merbach*, have led to new insights into the dynamics of Ln complexes, and some of the factors that govern water exchange in such complexes.

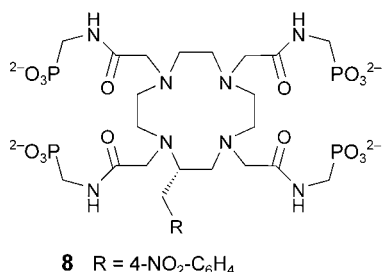
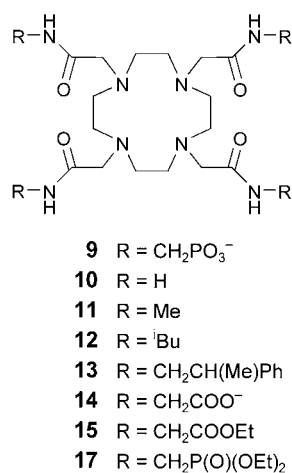
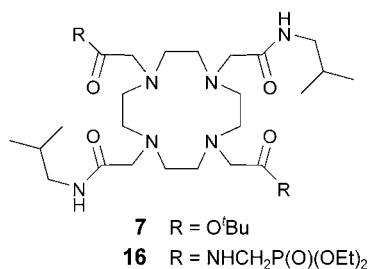
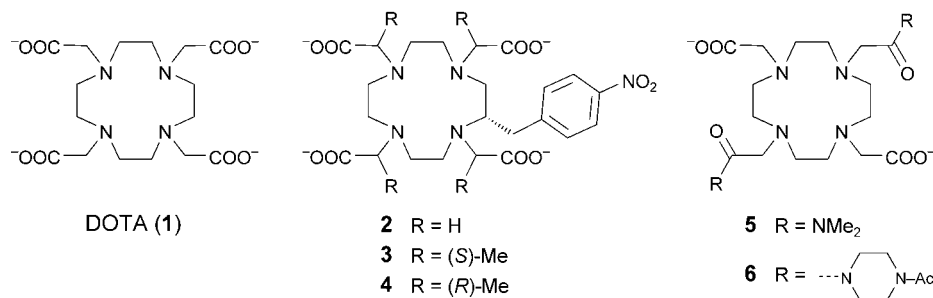
It has been estimated that relaxivity could be optimized by slowing the rotation of a Gd^{3+} complex if τ_M of that complex is on the order of 20–30 ns [2]. There have been numerous experimental attempts to arrive at this optimal water exchange rate, for instance by 1) introduction of a pyridine into a macrocyclic ring [13–16], 2) substitution of acetate pendent arms by more bulky methylene phosphonate arms [17], 3) insertion of additional CH_2 units into either the backbone or pendent arms of DTPA-like ligands [18–20], 4) new ligand design based upon tripodal complexes [21], and 5) ‘locking’ the chelate into a single coordination geometry having fast water exchange [22]. Each of these approaches has resulted in the production of complexes with more-favorable water exchange rates, yet nobody has successfully used one of these ‘optimized’ exchange systems to achieve the maximum relaxivity predicted by theory by simply attaching one of these systems to a slowly tumbling macromolecule. Clearly, these are dynamic systems, and other factors such as internal motions, bond rotations, or water exchange limitations (when a low-molecular-weight agent is attached to a larger protein), ultimately limit the observed relaxivity.

In the following discussion, we will compare a series of known and new complexes of Eu^{3+} , Gd^{3+} , and Dy^{3+} and the ligands **1–17** with respect to lifetime of water exchange and analytical method. The results are summarized in the *Table*.

The scientific curiosity about factors that control water exchange in Ln complexes has catalyzed new interest in more-slowly exchanging systems. *Aime et al.* [23] were the first to observe a separate $^1\text{H-NMR}$ signal for the bound water molecule in $[\text{Eu}^{\text{III}}(\mathbf{10})]^{3+}$, a system with a τ_M value of *ca.* 120 μs for the M-isomer¹). This was quickly followed by similar reports for other tetraamide derivatives, including the corresponding *N*-methylated compound **11** [24] (or the dimethyl variant thereof [24]) or the sterically more-crowded *N*-(2-phenylpropyl) analogue **13** [25]. The τ_M values of the M-isomers for this series of complexes seem to vary with increasing steric bulk of the amide pendent arms, increasing from 120 to 156 to 278 μs (in MeCN at 298 K) for $[\text{Eu}^{\text{III}}(\mathbf{10})]^{3+}$ [24][26], $[\text{Eu}^{\text{III}}(\mathbf{11})]^{3+}$ [24], and $[\text{Eu}^{\text{III}}(\mathbf{13})]^{3+}$ [25], respectively (*Table*).

However, factors other than steric bulk may also influence water exchange, as evidenced by the observation that a Eu^{3+} -bound water resonance has been detected in the high-resolution $^1\text{H-NMR}$ spectrum of $[\text{Eu}^{\text{III}}(\mathbf{15})]^{3+}$ in pure water at ambient temperature [27]. This observation led us to investigate the use of such systems to alter

¹) The so-called ‘M-isomer’ (not to be confused with the helicity descriptor *M*) refers to a square-antiprism geometry. Twisted-square-antiprism isomers, in turn, are commonly termed ‘m-isomers’ (not to be confused with the locant *m* for *meta*).



MRI contrast not by altering relaxation rates, but rather by changing the *intensity* of the bulk-water signal detected in the imaging experiment by means of a chemical-exchange-saturation-transfer (CEST) mechanism [28]. We and others have since shown that such complexes offer a new avenue in the design of 'smart' contrast agents, because chemical exchange in these systems is exquisitely sensitive to changes in pH [29–31], temperature [32], and metabolism [33][34]. Systems with a slow water exchange may offer another advantage in that one can then modulate prototropic exchange (rather than molecular exchange) to create a T_1 relaxation agent that responds to pH. This feature makes the water relaxivity of [Gd^{III}(**9**)]⁵⁻ highly pH-sensitive over the important physiological range [35][36]. Indeed, [Gd^{III}(**9**)]⁵⁻ has recently been used *in vivo* to map the distribution of tissue pH in functioning rat kidney [37] and in brain tumors (unpublished data).

Clearly, the tunability of the lifetime of Ln³⁺-bound water has become a focal point for many investigators interested in the development of novel, 'smart' MRI contrast

Table. *Characterization of Lanthanide Complexes of Type [Ln^{III}(L)]* (L = ligand). The ligands **1–17** (see chemical formulae) and the Ln³⁺ metal ions, the number of solution species¹) and their ratio, the solvents used, and the measured lifetimes τ_M of metal-bound water are given. All data refer to a temperature of 298 K; W = water.

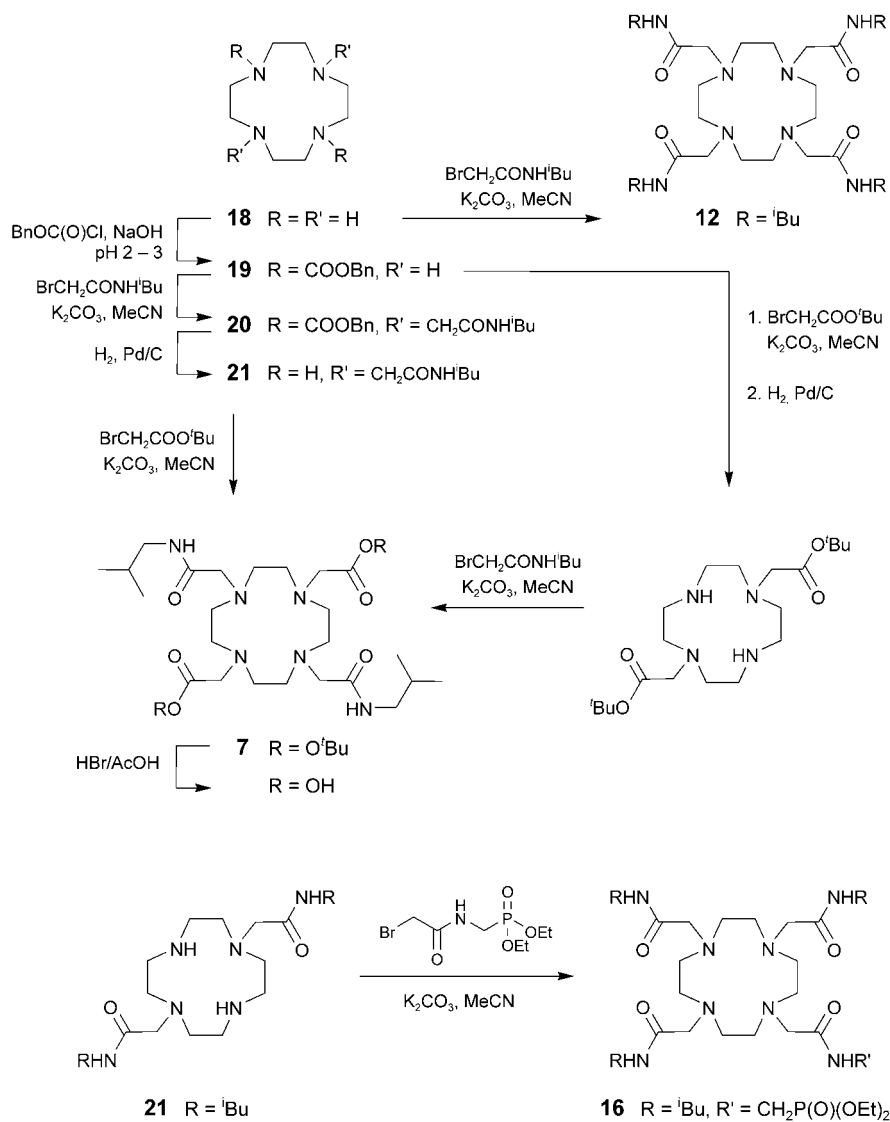
Ligand	Ln ³⁺	Species	M/m ¹)	Method	Solvent	τ_M [μ s]	Ref.
none	Gd		–	¹⁷ O-NMR	W	0.002	[8]
1	Eu	2	80:20	¹ H-NMR	W	–	[51]
1	Gd	2	–	¹⁷ O-NMR	W	0.240 ^a)	[5][52]
2	Gd	2	90:10	¹⁷ O-NMR	W	0.200 ^a)	[53]
3	Gd	1	–	¹⁷ O-NMR	W (pH 7)	0.120 (M)	[22]
4	Gd	1	–	¹⁷ O-NMR	W (pH 7)	0.015 (m)	[22]
5	Gd	2	60:40	¹⁷ O-NMR	W (pH 7)	1.35 ± 0.07 (M) 0.014 ± 0.001 (m)	[46]
6	Gd	2	83:17	¹⁷ O-NMR	W (pH 7)	2.35 ± 0.12 (M) 0.003 ± 0.001 (m)	[46]
7	Eu	1	–	¹ H-NMR ^b)	CD ₃ CN	10.0 ± 0.01 (M)	this work
8	Gd	1	–	<i>T</i> ₁ (¹ H)	W (pH 7)	1.27	this work
9	Gd	1	–	¹⁷ O-NMR	W (pH 7.2)	25.5 ± 0.5 (M)	this work
	Dy	1	–	¹⁷ O-NMR	W (pH 6–9)	21.2 ± 1.2 (M)	[35]
10	Eu	2	70:30	¹ H-NMR ^b)	CD ₃ CN	120 (M)	[23]
	Eu	2	–	CEST	W (pH 7)	2 (m) 89.5 ± 16.3 (M)	[42]
11	Eu	2	70:30	¹ H-NMR ^b)	CD ₃ CN	156 (M)	[26]
12	Eu	2	60:40	¹ H-NMR ^c)	CD ₃ CN	146 ± 5 (M)	this work
13	Eu	2	–	¹ H-NMR ^b)	CD ₃ CN	278 ± 1 (M)	[25]
14	Eu	1	–	¹ H-NMR ^b)	W (pH 7.4)	262 ± 1 (M)	[47]
15	Gd	1	–	<i>T</i> ₁ (¹ H)	W (pH 7)	190 ± 10	this work
	Gd			¹⁷ O-NMR	CD ₃ CN	250 ± 10	this work
	Eu			¹ H-NMR ^b)	W (pH 7)	369 ± 5 (M)	[27]
	Eu			¹ H-NMR ^b)	CD ₃ CN	789 ± 101 (M)	[27]
16	Eu	1	–	¹ H-NMR ^b)	CD ₃ CN	1254 ± 98 (M)	this work
17	Gd	1	–	<i>T</i> ₁ (¹ H)	W (pH 7)	805 ± 8	[36]
	Eu			¹ H-NMR ^b)	CD ₃ CN	1346 ± 6 (M)	[36]

^a) Average. ^b) Direct method. ^c) Saturation transfer.

agents that alter image contrast by either relaxation or a CEST mechanism. It is now known that τ_M in Ln complexes is exquisitely sensitive to both the size of the central metal cation [38] and the ligand structure [39]. *Merbach* has played a key role in the development of this field and, in celebration of his contributions, we wish to report some new data, and to review some older ones, for a series of selected di- and tetraamide ligands based on DOTA, as well as their complexes formed with Ln³⁺ ions.

2. Results and Discussion. – 2.1. *Synthesis of Modified DOTA Ligands.* The general procedures for the preparation of the ligands are summarized in the *Scheme*. Starting from cyclen (=1,4,7,12-tetraazacyclododecane; **18**), the corresponding tetraamide derivatives with four identical pendent arms were readily prepared by reaction with various *N*-alkyl or other 2-bromoacetamides in MeCN in the presence of a slight excess of K₂CO₃. However, a sequence of protection/deprotection steps was required to prepare mixed tetraamides with two types of pendent arms [40]. Typically, the 1,7-N-atoms of cyclen (**18**) can be selectively protected by reacting **18** with benzyl

Scheme. Synthesis of Modified DOTA Ligands



chloroformate and NaOH at *ca.* pH 2–3. This is then followed by alkylation of the remaining two N-atoms, followed by removal of the (benzyloxy)carbonyl protective groups by catalytic hydrogenation (H₂, Pd/C), and, finally, by addition of the second type of amide substituents.

2.2. *Determination of the Lifetime (τ_M) of Bound Water.* There are numerous NMR methods available for measuring τ_M for Ln-bound water, including variable-temperature (VT) ¹⁷O-NMR [1], *T*₁ nuclear-magnetic-relaxation-dispersion (NMRD) profiles

[41], VT- ^1H -NMR band-shape simulations [27], VT water-relaxivity measurements [27][36], and CEST spectral fitting [42]. Each method has its advantages and limitations. Several examples will be discussed below.

2.2.1. *VT- ^{17}O -NMR*. This method, widely applied by *Merbach* and colleagues [1], has proven effective in measuring τ_{M} over a wide range. It is especially effective for Ln complexes whose relaxation enhancement is relatively large (Gd, Dy, Tb, *etc.*), but ineffective for Ln complexes whose relaxation enhancement of the ^{17}O -NMR signal is small (Sm, Eu, Yb, *etc.*). The method is also less sensitive when τ_{M} for Ln $^{3+}$ -bound water is either too small (fast exchange) or too large (slow exchange). Examples of such extremes may be seen in the VT- ^{17}O -NMR curves for $[\text{Gd}^{\text{III}}(\mathbf{2})]^-$, $[\text{Gd}^{\text{III}}(\mathbf{4})]^-$, and $[\text{Gd}^{\text{III}}(\mathbf{9})]^{5-}$, as shown in *Fig. 1*. Obviously, the τ_{M} value for $[\text{Gd}^{\text{III}}(\mathbf{2})]^-$ can be more reliably determined because of the features presented by these data, *i.e.*, a characteristic point of inflection [22]. In contrast, the lifetimes of $[\text{Gd}^{\text{III}}(\mathbf{4})]^-$ and $[\text{Gd}^{\text{III}}(\mathbf{9})]^{5-}$ are less accurate due to their featureless ^{17}O -NMR curves (no point of inflection).

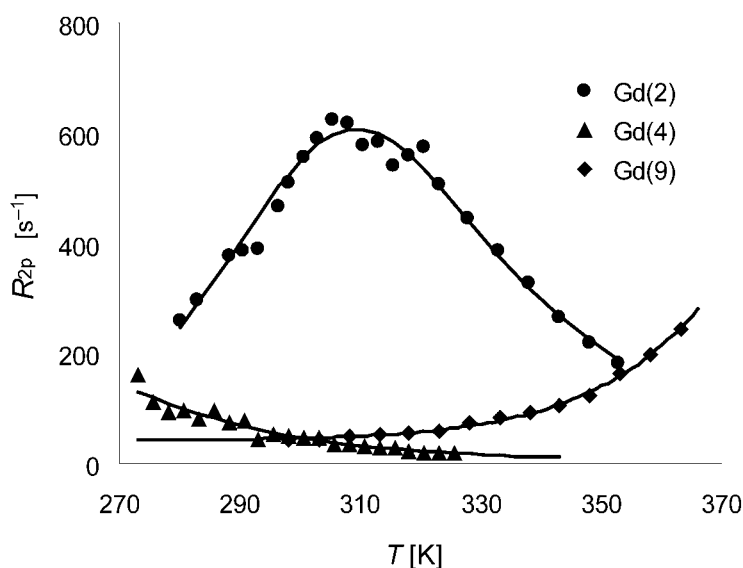


Fig. 1. Variable-temperature ^{17}O -NMR linewidth curves for $[\text{Gd}^{\text{III}}(\mathbf{2})]^-$, $[\text{Gd}^{\text{III}}(\mathbf{4})]^-$, and $[\text{Gd}^{\text{III}}(\mathbf{9})]^{5-}$. The curves were fitted to the *SBM* theory according to published procedures [12].

2.2.2. *Variable-Temperature ^1H -NMR Relaxation Time*. If the exchange of bound water is extremely slow, the inner-sphere contribution will be negligible at low temperatures, and will gradually increase at higher temperatures. Examples of this behavior from the literature include $[\text{Gd}^{\text{III}}(\mathbf{15})]^{3+}$ and $[\text{Gd}^{\text{III}}(\mathbf{17})]^{3+}$ [27][36]. Here, we show that $[\text{Gd}(\mathbf{8})]^{5-}$ presents a similar behavior (*Fig. 2*). By fitting the data to the standard *Solomon–Bloembergen–Morgan (SBM)* theory, a τ_{M} value of 1.27 μs was obtained. The advantage of this method is its relative simplicity, but it is suitable only for systems with τ_{M} values on the order of microseconds.

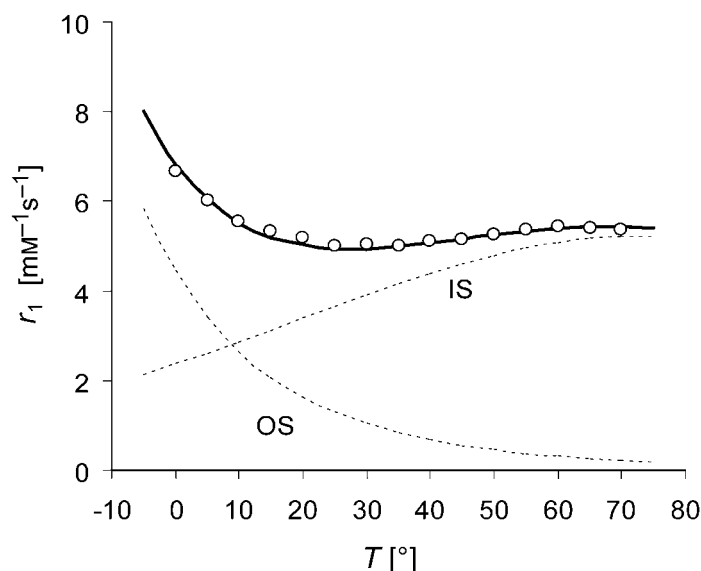


Fig. 2. Temperature dependence of the 20-MHz relaxivity of $[Gd^{III}(\mathbf{8})]^{3-}$ in aqueous solution at pH 7.0. The solid line reflects the best fit of the data to the SBM theory, the dotted lines show the individual outer-sphere (OS) and inner-sphere (IS) contributions [27][36].

2.2.3. *Saturation Transfer.* Magnetization-transfer techniques have historically found many applications in chemical and biological systems [43]. Recently, it has been found that the bound water molecule in a series of Eu complexes with DOTA tetraamides exchanges so slowly that a separate, highly shifted bound water signal could be directly observed by high-resolution $^1\text{H-NMR}$ [23–27]. This offers the opportunity to use an entirely different mechanism for producing image contrast based upon CEST. Paramagnetic versions of slow-chemical-exchange molecules are now referred to as PARACEST agents [44]. If chemical exchange in these systems meets the slow-to-intermediate exchange regime condition ($\Delta\omega \times \tau_M \gg 1$), then the degree of saturation of bulk water (M_t/M_0) will depend upon the chemical exchange rate (k_{obs}) and the relaxation properties of the system according to Eqn. 1.

$$\frac{M_t}{M_0} = \frac{1}{(1 + k_{\text{obs}} T_{\text{1sat}})} + \left[\frac{k_{\text{obs}} T_{\text{1sat}}}{(1 + k_{\text{obs}} T_{\text{1sat}})} \right] \exp \left[- \frac{(1 + k_{\text{obs}} T_{\text{1sat}})}{T_{\text{1sat}}} \times t \right] \quad (1)$$

Here, M_t and M_0 are signal intensities of bulk water with and without saturation at the exchanging site, respectively, for a period of time t ; T_{1sat} is the spin–lattice relaxation time of bulk water H-atoms during steady-state saturation at the bound-water site; k_{obs} is the pseudo-first-order exchange rate between bulk water and the H-atoms of bound water, equivalent to the concentration ratio of the bound-water site relative to bulk water, divided by the lifetime τ_M of the bound-water site. Thus, Eqn. 1 is an alternative way to measure τ_M of Ln complexes. An example of such data is given in

Fig. 3 for $[\text{Eu}^{\text{III}}(\mathbf{12})]^{3+}$. By adding different amounts of water (5–100 μl) to $[\text{Eu}^{\text{III}}(\mathbf{12})(\text{H}_2\text{O})]^{3+}(\text{CF}_3\text{SO}_3^-)_3$ (30 mg) in CD_3CN (0.4 ml), the relative concentrations of the bound and bulk pools change, and this is reflected by large differences in the equilibrium magnetization, M_t/M_0 , of bulk water at steady-state. Fitting of those data to Eqn. 1 gives an average τ_M value of $146 \pm 5 \mu\text{s}$, which is similar to values reported for other DOTA tetraamide complexes, as determined by other methods (Table). One should keep in mind that Eqn. 1 has an approximation of approaching steady-state, and assumes complete saturation of the bound pool. In practice, however, full saturation of the bound pool is experimentally difficult to achieve. Recently, we reported a numeric method for solving the modified Bloch equations that does not require such assumptions [42].

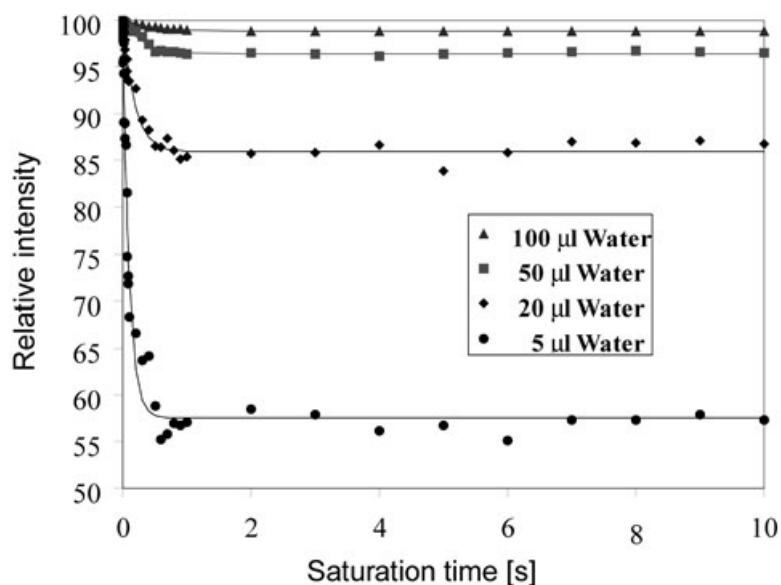


Fig. 3. $^1\text{H-NMR}$ Saturation-transfer experiments with $[\text{Eu}(\mathbf{12})(\text{H}_2\text{O})](\text{CF}_3\text{SO}_3^-)_3$. To a soln of the complex (30 mg) in anhydrous CD_3CN (0.4 ml) were added 5, 20, 50, or 100 μl of H_2O . The saturation frequency was set to the bound H_2O resonance (55 ppm rel. to bulk H_2O at 0 ppm), with a B_1 value of 1200 Hz and different saturation duration times (0–10 s). The experiments were performed on a Varian Inova-500 spectrometer with a PFG/ID probe. The solid lines reflect the fits of the data to Eqn. 1 (see text) for a τ_M value of $146 \pm 5 \mu\text{s}$.

2.3. Factors Affecting τ_M . 2.3.1. Lanthanide Coordination Geometry. Early NMR studies of the $[\text{Ln}^{\text{III}}(\text{DOTA})]^-$ complexes showed that two slowly interconverting species are present in aqueous solution, and that the populations of these two species are sensitive to the size of the central Ln^{3+} cation [45]. These two coordination isomers have since been assigned to the M- and m-isomers¹⁾ of square-antiprism and twisted-square-antiprism geometries, respectively, related to each other by rotation of the side-chain $\text{CH}_2\text{C}(\text{O})$ groups attached to the four central N-atoms of DOTA. Interestingly, it was subsequently discovered that these two species give rise to quite different τ_M values, the m-isomer showing much faster exchange compared to the M-isomer. For example, in the case of $[\text{Eu}^{\text{III}}(\mathbf{10})]^{3+}$, τ_M is 120 μs for the M-, but only 2 μs for the m-isomer

[23][24][26]. Analogously, values of 1.35 vs. 14 ns, and 2.35 vs. 3 ns were found for the M- and m-isomers of $[\text{Gd}^{\text{III}}(\mathbf{5})]^+$ and $[\text{Gd}^{\text{III}}(\mathbf{6})]^+$, respectively [46]. Such dramatic differences were recently confirmed by the successful separation and characterization of the M- and m-isomers of the same molecule differing only in chirality ($\tau_{\text{M}} = 120$ ns for $[\text{Gd}^{\text{III}}(\mathbf{3})]^-$ vs. 15 ns for $[\text{Gd}(\mathbf{4})]^-$) [22].

2.3.2. *Complex Rigidity.* Ligands **2** and **3** differ from DOTA (**1**) by an additional 4-nitrobenzyl group on the macrocyclic backbone (for **2**), or by a combination of backbone substituents including Me groups in the α -positions of the pendant arms (for **3**). This provides ligands with increasing rigidities in the series $[\text{Gd}^{\text{III}}(\mathbf{1})]^- < [\text{Gd}^{\text{III}}(\mathbf{2})]^- < [\text{Gd}^{\text{III}}(\mathbf{3})]^-$. Interestingly, the measured τ_{M} values for this series decrease with increasing rigidity [τ_{M} values of 240 μs with ligand **1** (average of two coordination isomers), 200 ns with **2** (average of two coordination isomers), and 120 ns with **3** (single M-isomer)]. This indicates that water exchange becomes faster when the ligand architecture is rigidified by substitution. One could argue that the τ_{M} values reported for the Gd complexes with **1** and **2** have an exchange component that partially reflects the presence of the faster-exchanging m-isomer; so the differences described above may be even larger if exchange could be measured for the pure M-isomer in each case. A second illustration of this is provided by the complexes $[\text{Gd}^{\text{III}}(\mathbf{8})]^{5-}$ and $[\text{Gd}^{\text{III}}(\mathbf{9})]^{5-}$. Here, water exchange in the less-rigid complex with ligand **9** is *ca.* 20-times slower than in the more-rigid complex with **8** ($\tau_{\text{M}} = 26$ vs. 1.3 μs , resp.). This limited series may provide a better indicator of the effects of rigidity, because, in this case, both complexes exist nearly exclusively as the M-isomers.

2.3.3. *Side Chains of Ligands.* The data summarized in the *Table* reveal that other chemical characteristics of the extended amide side chains, especially polarity and charge, also affect τ_{M} , even though they are not typically involved in coordination to the central Ln ion. In general, for $[\text{Eu}^{\text{III}}(\text{DOTA-tetraamide})]$ complexes, τ_{M} correlates with the polarity of the ligand side chains, *i.e.*, phosphonates \geq carboxylates \gg alkyl groups \geq simple amides. For example, the measured τ_{M} values for one such series falls in the order $[\text{Eu}^{\text{III}}(\mathbf{17})]^{3+}$ (1.3 ms) [36] \geq $[\text{Eu}^{\text{III}}(\mathbf{16})]^{3+}$ (1.25 ms) $>$ $[\text{Eu}^{\text{III}}(\mathbf{15})]^{3+}$ (780 μs) [27] \gg $[\text{Eu}^{\text{III}}(\mathbf{13})]^{3+}$ (278 μs) [25] $>$ $[\text{Eu}^{\text{III}}(\mathbf{12})]^{3+}$ (146 μs) and $[\text{Eu}^{\text{III}}(\mathbf{11})]^{3+}$ (156 μs) [24] $>$ $[\text{Eu}^{\text{III}}(\mathbf{10})]^{3+}$ (120 μs) [23], as determined in each case for the corresponding M-isomers in hydrous MeCN solution. A correlation between τ_{M} and a calculated water-accessibility parameter has been reported for an even more-extensive series of Eu^{3+} complexes [39].

Complexes with negatively charged side chains generally display lower τ_{M} values than their neutral counterparts. For example, the τ_{M} values of $[\text{Eu}^{\text{III}}(\mathbf{5})]^+$ and $[\text{Eu}^{\text{III}}(\mathbf{6})]^+$ (1.3–2.3 μs) are *ca.* five times smaller than that of $[\text{Eu}^{\text{III}}(\mathbf{7})]^{3+}$ (10 μs); and the τ_{M} value measured for $[\text{Gd}^{\text{III}}(\mathbf{9})]^{5-}$ (25 μs , at pH 7.2) is notably smaller than that of the corresponding ester, $[\text{Gd}^{\text{III}}(\mathbf{17})]^{3+}$ (805 μs , at pH 7.4). Similarly, the τ_{M} value found for $[\text{Eu}^{\text{III}}(\mathbf{14})]^-$ (262 μs , pH 7.4) is somewhat lower than the one for the corresponding ester, $[\text{Eu}^{\text{III}}(\mathbf{15})]^{3+}$ (382 μs , pH 7.4) [27][47].

2.4. *Molecular vs. Prototropic Exchange.* Aime *et al.* [48] recently published a review article on the relaxivity contributions from the prototropic exchange vs. exchange of water in Gd^{3+} complexes. It has been observed that prototropic exchange is accelerated in complexes of the type discussed here in the presence of acids and/or bases, and that an increase in prototropic exchange results in an increase in relaxivity below and above

ca. pH 2 and 9–10, respectively [49]. This early observation prompted us to examine more-closely the water relaxivity of $[\text{Gd}^{\text{III}}(\mathbf{9})]^{5-}$ as a function of pH. In this interesting, pH-sensitive complex, the ^1H relaxivity of water steadily increases between pH 8.5 ($r_1 = 4.5 \text{ mM}^{-1} \text{ s}^{-1}$) and pH 6 ($r_1 = 9.8 \text{ mM}^{-1} \text{ s}^{-1}$) [35]. It has been shown that this effect is not due to an increase in the exchange of water molecules over this pH range [35], but is rather due to an increase in prototropic-exchange rate catalyzed by the appended phosphonate groups. The phosphonate groups in this complex undergo four distinct protonations between pH 8.5 and 6. This implies that the monoprotonated species, with a single PO_3H^- function, are most efficient at catalyzing proton exchange between the Gd^{3+} -bound water H-atoms and bulk solvent. Such pH-dependent relaxivities are not a feature of current clinical Gd^{3+} -based contrast agents, where water exchange is relatively fast ($\tau_M < 240 \text{ ns}$), so the retarded exchange feature of $[\text{Gd}^{\text{III}}(\mathbf{9})]^{5-}$ makes this complex an attractive agent for mapping extracellular pH in tissues by MRI [37].

2.5. Size of the Metal Cation. *Merbach* and co-workers [12] found for a series of $[\text{Ln}(\text{DTPA})(\text{BMA})]$ complexes that the metal-bound water lifetimes τ_M decrease from $1.88 \mu\text{s}$ (Nd^{3+}) to $0.16 \mu\text{s}$ (Ho^{3+}) and suggested that this reflects a change in water exchange mechanism from interchange (I_a) to dissociative (D) type upon going from larger towards smaller cations. More recently, *Parker* and co-workers [25] reported that the τ_M value of $[\text{Eu}^{\text{III}}(\mathbf{13})]^{3+}$ might be as much as 500 times higher than that of the corresponding Yb^{3+} complex. We have also observed that the τ_M values vary dramatically with Ln ionic radii for the $[\text{Ln}^{\text{III}}(\mathbf{15})]^{3+}$ series [38]. It is especially interesting that the τ_M values in $[\text{Eu}^{\text{III}}(\mathbf{15})]^{3+}$ [27] and $[\text{Eu}(\mathbf{17})]^{3+}$ [36] are about twice as high as those of the corresponding Gd^{3+} complexes, even though Eu^{3+} and Gd^{3+} complexes are usually considered isostructural because of their similar ionic radii (0.95 and 0.94 \AA , respectively).

2.6. Solvent Effects. The data summarized in the *Table* also indicate that the lifetimes of Ln^{3+} -bound water for identical complexes measured in hydrous MeCN *vs.* bulk water may differ substantially. For example, τ_M values of 789 *vs.* $369 \mu\text{s}$, and 120 *vs.* $89 \mu\text{s}$, have been determined for $[\text{Eu}^{\text{III}}(\mathbf{15})]^{3+}$ and $[\text{Eu}^{\text{III}}(\mathbf{11})]^{3+}$, respectively, in MeCN *vs.* water [27]. This may be related to the solvent accessibility, as suggested previously [39], or reflect a larger contribution from prototropic exchange in bulk water. Given that the mechanism of water exchange in these tetraamide complexes occurs *via* a D -mechanism, greater solvent accessibility to the Eu^{3+} -bound water molecule may aid dissociation of the bound water by H-bonding with bulk water.

Conclusions. – Water exchange has arguably become the most-interesting physical parameter in Ln complexes that may be manipulated by clever chemistry and used to advantage in MRI applications. We have summarized in this article the NMR methods used to measure water exchange, and have highlighted the influence of complex charge, ionic radius of the central metal, solvent accessibility, coordination geometry, and molecular rigidity on the lifetimes τ_M of inner-sphere bound water. It is now possible to design Ln complexes that display τ_M values ranging over six orders of magnitude, *i.e.*, from nano- to milliseconds.

The following general observations can be made: 1) $[\text{Ln}(\text{DOTA-tetraamide})]$ complexes have much higher τ_M values compared to $[\text{Ln}(\text{DOTA-diamide})]$ complexes; 2) additional charged functional groups on the pendent amide arms reduce the τ_M

values greatly, even though they may not be directly involved in coordination to the central Ln cation; 3) τ_M values are very sensitive to the ionic radius of the central Ln ion, and can even vary for ions with very similar ionic radii such as Eu^{3+} and Gd^{3+} ; and 4) the solvent obviously influences water exchange in these complexes. For $[\text{Eu}^{\text{III}}(\text{DOTA-tetraamide})]$ complexes, the lifetime of bound water is typically ca. twice as fast in bulk water compared to hydrous MeCN. Hopefully, these observations may be helpful in design of new Ln-based contrast agents for MRI that have optimal dynamic properties for either fast (Gd-based relaxivity) or slow (other Ln-based CEST) contrast applications.

This work was supported by Grants from the NIH (RR-02584 and CA 84697), the Robert A. Welch Foundation (AT-584), and the Texas Advanced Technology Program (ATP).

Experimental Part

The following chemicals and solvents were purchased from Sigma-Aldrich (Milwaukee, WI), and used without further purification: benzyl chloroformate, isobutylamine, bromoacetyl bromide, *tert*-butyl bromoacetate, diisopropyl(ethyl)amine, 10% Pd/C, 1,4-dioxane, anhydrous MeCN, anhydrous Et_2O , and anhydrous EtOH. Cyclen (= 1,4,7,12-tetraazacyclododecane; **18**) was purchased from Strem Chemicals (Newburyport, MA). Ligand **8** (and the corresponding Gd^{III} complex) was synthesized by Fredrick Tajada (Ph.D. Thesis, University of Texas at Dallas, 2002). Column chromatography (CC) was performed with SilicAR-150 silica gel (60–200 mesh; Mallinckrodt). Hydrogenations were performed in a Parr hydrogenation apparatus. NMR Data: δ in ppm rel. to Me₄Si as internal standard.

2-Bromo-N-(2-methylpropyl)acetamide (reagent for the synthesis of **7**, **12**, and **16**). In a N_2 -purged, three-neck 100-ml flask, isobutylamine (4.97 ml, 0.05 mol) was dissolved in benzene (60 ml), and K_2CO_3 (8.293 g, 0.05 mole) was added. Bromoacetyl bromide (4.36 ml, 0.05 mol) was added dropwise over 30 min, while maintaining the temp. at 0° . The mixture was then warmed to r.t. and stirred overnight. The solids were removed by filtration, and the solvent was evaporated under reduced pressure. The remaining residue was dissolved in Et_2O (20 ml), washed with H_2O (3×20 ml), and the combined org. extract was dried (Na_2SO_4) overnight. The remaining solid was removed by filtration, and the solvent was evaporated *in vacuo* to afford colorless crystals (7.77 g) in 80% yield. $^{13}\text{C-NMR}$ (75 MHz, CDCl_3): 165.42 (C=O); 47.51 (NHCH₂); 29.51 (BrCH₂); 28.40 (CH); 20.05 (2 Me).

N,N',N'',N'''-Tetrakis(2-methylpropyl)-1,4,7,10-tetraazacyclododecane-1,4,7,10-tetraacetamide (12). To a soln. of cyclen (**18**; 0.86 g, 0.005 mol) in MeCN (20 ml) were added 2-bromo-N-(2-methylpropyl)acetamide (3.88 g, 0.020 mol) and K_2CO_3 (3.0 g, 0.022 mol). The mixture was heated at $60-70^\circ$ overnight. The resulting solid was removed by filtration, CHCl_3 was added, and the mixture was heated to reflux. The soln. was concentrated and cooled to yield **12** (2.86 g, 91%). Colorless solid. $^1\text{H-NMR}$ (270 MHz, CDCl_3): 6.97 (*t*, NH); 3.05 (*s*, CH_2CO); 2.70 (*s*, CH_2CH_2); 1.75 (*m*, CH); 0.88 (*d*, Me). $^{13}\text{C-NMR}$ (75 MHz, CDCl_3): 170.69 (C=O); 57.83 (NHCH₂); 50.20 (CH₂ (ring)); 46.24 (CH₂NH); 28.26 (CH); 19.70 (Me).

Bis(phenylmethyl) 1,4,7,10-tetraazacyclododecane-1,7-dicarboxylate (19). Prepared according to a literature procedure [40].

Bis(phenylmethyl) 4,10-Bis[2-[(2-methylpropyl)amino]-2-oxoethyl]-1,4,7,10-tetraazacyclododecane-1,7-dicarboxylate (20). In a 100-ml three-neck flask, **19** (2.2 g, 0.005 mol) was dissolved in MeCN (20 ml). Then, $\text{Et}(\text{i-Pr})_2\text{N}$ (1.5 g) in MeCN (7 ml) was added at 0° , followed by 2-bromo-N-(2-methylpropyl)acetamide (2.13 g, 0.011 mol) in MeCN (7 ml). The mixture was stirred at 0° for 2 h, then warmed to 60° , and stirred for an additional 20 h at this temp. The solvent was removed, and the residue was partitioned between Et_2O (100 ml) and H_2O (20 ml). The org. layer was washed with H_2O (2×20 ml) and 5% aq. NaOH soln. (2×20 ml). The org. layer was dried (Na_2SO_4) overnight. The solvent was removed *in vacuo* to afford the crude product as light-yellow oil, which was purified by CC (SiO_2 ; Et_2O) to yield the title compound as a colorless oil (2.73 g, 82%). $^1\text{H-NMR}$ (270 MHz, CDCl_3): 7.28 (*m*, arom. H); 5.02 (*s*, COOCH_2); 3.42, 2.73 (CH₂ (ring)); 3.38 (NCH₂); 3.12 (NHCH₂); 2.96 (*br.*, NH); 1.71 (*br.*, CH); 0.83 (*d*, Me). $^{13}\text{C-NMR}$ (75 MHz, CDCl_3): 170.95 (CH_2CO); 156.85 (COO); 136.31, 128.68, 128.38, 128.19 (arom. C); 67.51 (NCH₂); 58.85 (OCH₂); 55.94, 48.51 (CH₂ (ring)); 46.66 (NHCH₂); 28.58 (CH); 20.31 (Me).

N,N'-Bis(2-methylpropyl)-1,4,7,10-tetraazacyclododecane-1,7-diacetamide (**21**). Compound **20** (see above; 1.1 g, 1.65 mmol) was dissolved in anhyd. EtOH (20 ml), and 10% Pd/C (200 mg) was added. The mixture was hydrogenated at 20–25 psi for 48 h. The catalyst was filtered off, and the solvent was removed *in vacuo* to afford **21** as a colorless oil (0.643 g, 98%). ¹H-NMR (270 MHz, CDCl₃): 7.57 (t, NHCH₂); 7.19 (br., NH); 3.20 (s, CH₂CO); 2.90 (dd, CH₂); 2.70 (br., CH₂ (ring)); 1.65 (m, CH); 0.72 (d, Me). ¹³C-NMR (75 MHz, CDCl₃): 171.32 (C=O); 59.91 (NCH₂); 52.65 (CH₂ (ring)); 46.85 (CH₂ (ring)); 46.62 (NHCH₂); 28.37 (CH); 20.29 (Me).

Tetraethyl [(4,10-Bis[2-[(2-methylpropyl)amino]-2-oxoethyl]-1,4,7,10-tetraazacyclododecane-1,7-diyl)-bis[(1-oxo-2,1-ethanediy)iminomethylene]]bis(phosphonate) (**16**). To a soln. of **21** (0.643 g, 1.61 mmol) in anhyd. MeCN (10 ml) were added K₂CO₃ (0.446 g) and diethyl [(bromoacetyl)amino]methylphosphonate (0.930 g, 3.23 mmol) [50]. The mixture was stirred at 40° for 14 h, and then at 60° for 8 h. The solvent was removed on a rotary evaporator, and the residue was partitioned between Et₂O (20 ml) and H₂O (10 ml). The org. layer was washed with H₂O (2 × 10 ml), 5% aq. NaOH soln. (10 ml), and H₂O (2 × 10 ml), dried (Na₂SO₄) overnight, and evaporated *in vacuo* to afford **16** (0.821 g, 63%). ¹³C-NMR (75 MHz, CDCl₃): 171.44 (C=O); 170.90 (C=O); 62.71 (CH₂ Me); 60.17 (NCH₂); 58.29 (NCH₂); 54.32, 52.93 (CH₂ (ring)); 46.47 (CH₂CH); 34.63 (d, CH₂P); 28.57 (CH); 20.27 (Me); 16.53 (CH₂Me).

Bis(1,1-Dimethylethyl) 10-Bis[2-[(2-methylpropyl)amino]-2-oxoethyl]-1,4,7,10-tetraazacyclododecane-1,7-diacetate (**7**). Compound **21** (0.485 g, 1.22 mmol) was alkylated with *tert*-butyl bromoacetate (0.475 g, 2.44 mmol) in the presence of K₂CO₃ (0.337 g), as described above, to afford **7** (0.598 g) as a pale yellow oil. ¹³C-NMR (75 MHz, CDCl₃): 171.49 (C=O); 170.92 (C=O); 50–52 (CH₂ (ring)); 57.95 (NCH₂); 56.18 (NCH₂); 46.24 (NHCH₂); 28.28 (Me₂CH); 19.66 (Me₂CH), 81.15 (CMe₃); 27.52 (CMe₃).

Lanthanide Complexes. The complexes were synthesized by mixing the appropriate macrocyclic ligand with a lanthanide chloride (or triflate) in either MeCN or water according to established procedures [27].

NMR Spectroscopy and Data Analysis. Longitudinal-relaxation measurements for water H-atoms were performed with an MRS-6 analyzer operating at 20 MHz (Institut Jozef Stefan, Ljubljana, Slovenia) and an inversion-recovery pulse sequence (15 experiments, eight scans). The experiments were conducted under thermostated conditions (±0.5°) by means of an air-flow heater equipped with a copper thermocouple, and measured with an Omega CN76000 microprocessor-based temperature/processor controller. The NMR samples were allowed to equilibrate for 10 min at each temp. before data acquisition.

¹H- and ¹³C-NMR spectra of all ligands were recorded on a JEOL Eclipse-270 spectrometer. Variable-temperature (VT) ¹H-, ¹³C-, and ¹⁷O-NMR spectra were recorded on a Varian INOVA-500 spectrometer at 500, 125.6, and 67.8 MHz, respectively. Again, the probes were allowed to equilibrate for at least 10 min before data acquisition. An NMR band-shape analysis of the Ln³⁺-bound and bulk water resonances was performed by means of a program written in Fortran 77 for a two-site exchange system with unequal populations. The molar ratios of bound vs. bulk water were determined directly from the low-temperature ¹H-NMR integration values. The VT-¹⁷O-NMR linewidth data were fitted by following procedures published by Merbach and co-workers [12].

REFERENCES

- [1] 'The Chemistry of Contrast Agents in Medical Magnetic Resonance Imaging', Eds. A. E. Merbach, É. Tóth, John Wiley & Sons, Chichester, 2001, p. 471.
- [2] S. Aime, M. Fasano, E. Terreno, *Chem. Soc. Rev.* **1998**, 27, 19.
- [3] E. T. Ahrens, U. Rothbächer, R. E. Jacobs, S. E. Fraser, *Proc. Natl. Acad. Sci. U.S.A.* **1998**, 95, 8443.
- [4] K. Micskei, L. Helm, E. Brücher, A. E. Merbach, *Inorg. Chem.* **1993**, 32, 3844.
- [5] D. H. Powell, G. González, V. Tissières, K. Micskei, E. Brücher, L. Helm, A. E. Merbach, *J. Alloys Compd.* **1994**, 207–208, 20.
- [6] C. Cossy, L. Helm, A. E. Merbach, *Inorg. Chem.* **1988**, 27, 1973.
- [7] C. Cossy, L. Helm, A. E. Merbach, *Inorg. Chem.* **1989**, 28, 2699.
- [8] K. Micskei, D. H. Powell, L. Helm, E. Brücher, A. E. Merbach, *Magn. Reson. Chem.* **1993**, 31, 1011.
- [9] D. H. Powell, A. E. Merbach, *Magn. Reson. Chem.* **1994**, 32, 703.
- [10] P. Caravan, J. J. Ellison, T. J. McMurry, R. B. Lauffer, *Chem. Rev.* **1999**, 99, 2293.
- [11] V. Comblin, D. Gilsoul, M. Hermann, V. Humblet, V. Jacques, M. Mesbahi, C. Sauvage, J. F. Desreux, *Coord. Chem. Rev.* **1999**, 185–186, 451.
- [12] D. Pubanz, G. Gonzalez, D. H. Powell, A. E. Merbach, *Inorg. Chem.* **1995**, 34, 4447.

